



ARTICLE

Bio-Inspired Gelatin-Based Adhesive Modified with Waterborne Polyurethane on Click Chemistry

Xuechuan Wang^{1,2}, Wenying Zhao^{1,2}, Xugang Dang^{1,2,*}, Yiqing Wang^{1,2} and Huijie Zhang^{1,2,*}

¹College of Bioresources Chemical and Materials Engineering, Shaanxi University of Science and Technology, Xi'an, 710021, China

²National Demonstration Center for Experimental Light Chemistry Engineering Education, Shaanxi University of Science and Technology, Xi'an, 710021, China

*Corresponding Authors: Xugang Dang. Email: xg.dang@sust.edu.cn; Huijie Zhang. Email: hjzhang@sust.edu.cn

Received: 20 January 2022 Accepted: 09 March 2022

ABSTRACT

As a non-toxic, highly reactive biomass material, gelatin is widely used as the component of biomass-based adhesive. However, like most aqueous adhesives, gelatin-based adhesives suffer from long solidifying time or high solidifying temperature due to the low volatility of water, which highly limits the application potential of gelatin-based adhesives. Inspired by the fast adhesion of marine organisms through the formation of chemical crosslinks, herein, a kind of low temperature curable eco-friendly gelatin-based adhesive with good adhesive properties and fast curing at low temperature is developed by introducing clicking chemical Diels-Alder (DA) reaction between blocked waterborne polyurethane (MWPU) and gelatin. The furfuryl glycidyl ether (FGE) and 4-Maleimidophenol (4-HPM) for the DA reaction are grafted on gelatin, and the end-capping of MWPU, respectively. With the addition of MWPU and FGE, the cross-linking degree of gelatin increased, and the adhesion properties of the adhesive were improved. The shear strength and T-peel strength of the modified adhesive reached 0.95 MPa and 1.42 N/mm, respectively, after the curing time of 8 min at 40°C, which can meet the application requirements as adhesive for bio-medical use.

KEYWORDS

Gelatin; blocked waterborne polyurethane; eco-friendly adhesive; skin solid wastes

1 Introduction

With the development of the social economy and the increasing variety of leather products, China has become the center for leather production and consumption. However, leather processing yields around 17–20% of solid waste, including hides and skins [1]. Those leather wastes contained a large amount of collagen. Traditional disposal methods such as landfilling and incineration, not only occupied land resources but also caused a serious waste of collagen resources [2]. Fortunately, the collagen in skin waste could be readily hydrolyzed to obtain gelatin. As a biomass material, gelatin had the advantages of biocompatibility, non-toxicity, vast source, and low cost [3–5]. Gelatin was used in various fields, such as food packaging [6–8], tissue engineering [9–11], drug delivery [12–14], adhesives [15–17], and so on. Among those applications, adhesives were considered the most promising application direction for the gelatin extracted from skin waste. At present, the use of adhesives in various areas is in greater demand.

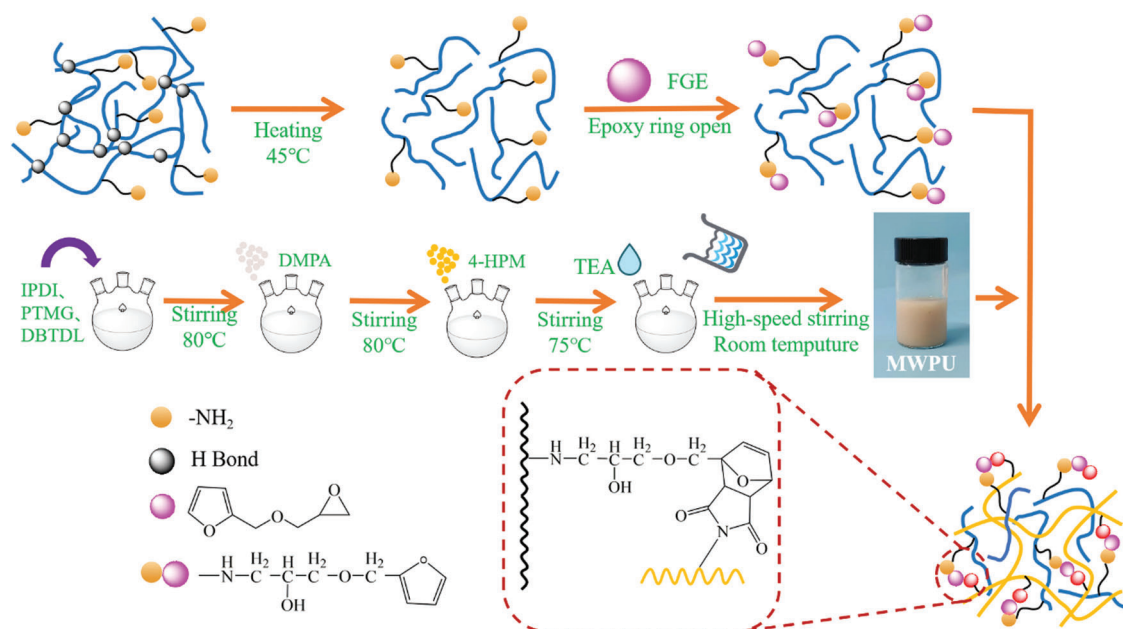


In the field of adhesives, eco-friendly adhesives were highly demanded. Gelatin is one of the most preferred materials due to its own non-toxic, and readily available in the skin industry. For adhesives, excellent adhesion properties, weather resisting property, fast-drying at relatively low temperature, and better adaptability to a variety of materials (skin, synthetic leather, rubber, and so on) are required. The presence of many hydrophilic groups ($-\text{COOH}$, $-\text{NH}_2$, $-\text{OH}$, and $-\text{CO}-\text{NH}-$) on gelatin led to poor water resistance and brittle film formation [18]. Generally, graft copolymerization [19,20] and cross-linking [21,22] modification were the most common and efficient modification methods to improve the water resistance and mechanical properties of modified gelatin. However, all these gelatin-based adhesives are rigid after solidification and require a long curing time or high curing temperature ($<80^\circ\text{C}$), which highly limited their application as adhesives. At present, gelatin-based adhesives are mainly applied to rigid materials with higher thermal stability like wood. In our previous work, the epoxy-terminated hyperbranched polymers (EHPAE) were used as a cross-linking agent to modify the gelatin (GE) in skin solid waste to synthesize an environmentally friendly adhesive based on gelatin with relatively high flexibility which can match the flexible skin. However, the complex synthesis process of the EHPAE and its high curing temperature limited its application as adhesives [23].

Polyurethane (PU) adhesive was one of the crucial types of adhesives. PU had different soft segments and hard segments, and it played an essential role in the manufacturing industry by adjusting the ratio structure of soft segments and hard segments and changing the properties of polyurethane to meet different requirements [24,25]. Aside from the organic solvent-based PU adhesives, waterborne polyurethane (WPU) adhesives with water as the primary dispersion medium attract growing attention due to their environmental friendliness [26]. Due to the high reactivity of the $-\text{NCO}$ group on WPU, and the facile synthesis process, the WPU has been used to modify gelatin to improve its water resistance. Dang et al. [27] grafted gelatins with waterborne polyurethane to prepare porous scaffold material (PEUR-g-GH). The synthesized PEUR-g-GH had good film-forming properties, water resistance, and thermal stability, and was cross-linking to form an excellent support bearing capacity. It showed that the water resistance of gelatin was highly improved after being grafted with the PEUR. However, the WPU based adhesive also suffers from the long curing time or high curing temperature, as the high unblocking temperature of $-\text{NCO}$ groups ($>110^\circ\text{C}$) eliminates the possibility cure the adhesives with the high reactive $-\text{NCO}$ ahead of waiting for the evaporation of water [28–30].

Click chemistry was well known for its fast reaction and was introduced into organic synthesis by Sharpless in 2001 [31]. The Diels-Alder reaction (DA cycloaddition) was one of the most critical clicks chemistry reactions. It was a $[4 + 2]$ cycloaddition reaction between diene compounds and dienophiles to form cyclohexene with substituent group [32,33]. The DA cycloaddition reaction had mild reaction conditions, few side reactions, thermal reversibility, and no need for additional catalysts [34]. The response could occur between 25°C and 120°C [35]. At present, these characteristics have enabled the DA reaction to being well studied in biomedical materials [36,37] and self-healing materials [38,39]. It was mainly used for preparing complex polymer networks such as hydrogels [40,41] and plastics [42,43].

Herein, the unique properties of click chemistry were used to accelerate the curing process at a low temperature of the gelatin-based adhesives. As shown in Scheme 1, gelatin extracted from the skin waste and the blocked waterborne polyurethane were used as the adhesive matrix in this study. The furan and maleimide groups for the DA cycloaddition reaction were grafted on gelatin and end-capped on MWPU, respectively. The modified MWPU and gelatin were mixed to form an adhesive. As the DA reaction enables the fast curing of the adhesive at moderate temperature. The research would be helpful to the utilization of biomass resources and accorded with the development of novel adhesives.



Scheme 1: Synthetic strategy of MWPU-FGE/GE adhesive

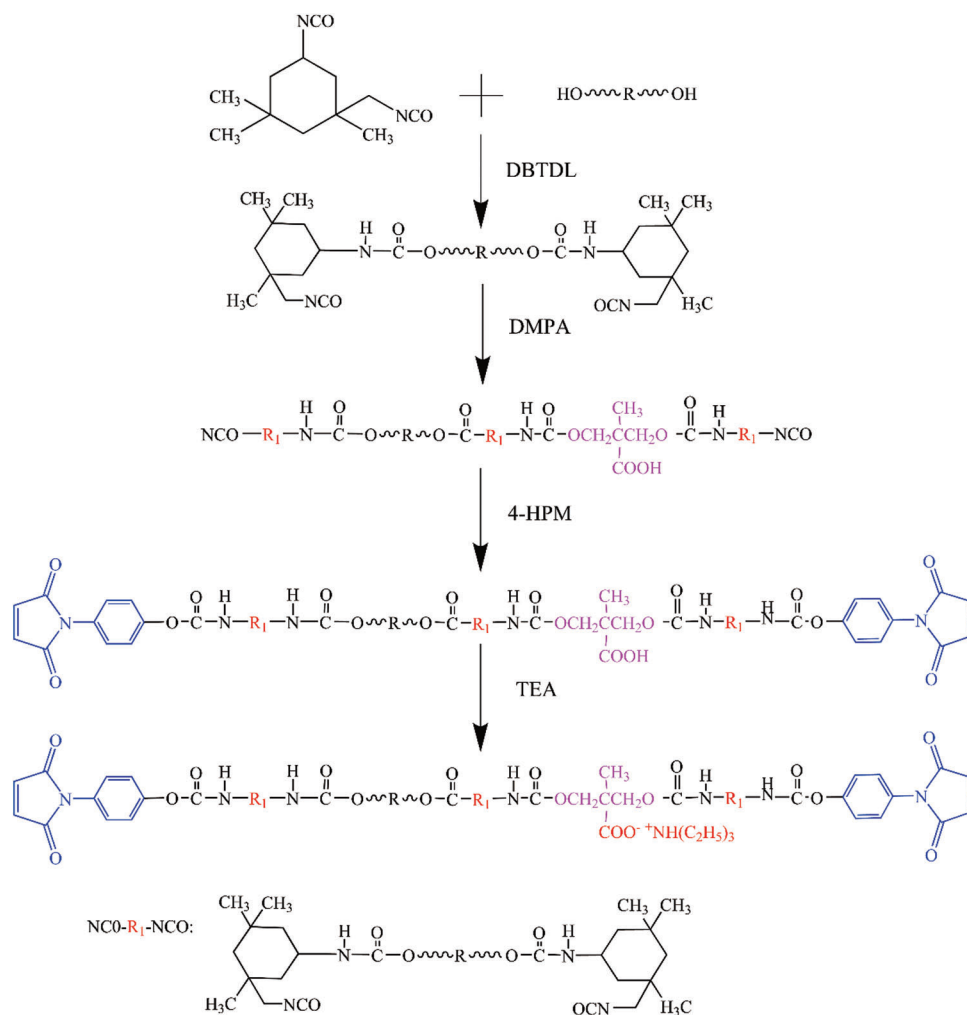
2 Experimental

2.1 Materials

Poly (tetramethylene glycol) (PTMG, $M_n = 1000$, purity 99%) was dried under vacuum at 80°C for 24 h before use. PTMG, Isophorone diisocyanate (IPDI, 99%), 2,2-Bis (hydroxymethyl) propionic acid (DMPA, 98%), 4-Maleimidophenol (4-HPM, 98%), Acetone (Ac), Triethylamine (TEA, 99%), Tetrabutylammonium hydrogen sulfate (98%), Furfuryl alcohol (FA, 98%), Sodium hydroxide (NaOH, 98%) and Diethyl ether anhydrous (99%) were purchased from Macklin Biochemical Co., Ltd. (Shanghai, China). Dibutyltin dilaurate (DBTDL, 99%), Epichlorohydrin (ECH, 99%), and Sodium dodecyl sulfate (SDS, AR) were purchased from Kermel Chemical Reagent Co., Ltd. (Tianjin, China). Gelatin (GE) extracted from leather solid wastes, was purchased from Henan Boyang Biotechnology Co., Ltd. (Henan, China). All reagents except GE were analytical grade. All reagents were used without further purification. The skins were bought from Henan Prosper & Colomer Munmany Co., Ltd. (China).

2.2 Preparation of the MWPU

The experiment was conducted in a 250 mL, three-necked round bottom flask with a condenser, a mechanical stirrer, and an N_2 inlet. When the temperature reached 80°C, the IPDI (4.00 g, 18 mmol), PTMG (10.00 g, 10 mmol), and a small amount of DBTDL were added and reacted for 2 h under the proper stirring. After this, DMPA (0.70 g, 5.2 mmol) and Ac (adjust the system viscosity) in suitable amounts were introduced, and the reaction was kept for 3 h. Then, when the mixture was cooled to 75°C, 4-HPM (0.56 g, 2.9 mmol) was added to block the reaction. Finally, TEA (0.53 g, 5.2 mmol) dissolved in distilled water (60 mL) then added and reacted for 1.5 h under the high-speed stirring. Exploring the different R values (the ratio of the amount of $-NCO$ in IPDI and the amount of $-OH$), DMPA content (wt.%, based on the weighted sum of IPDI and PTMG), 4-HPM content (% based on the amount of theoretical $-NCO$) and TEA content (% based on the amount of DMPA) on MWPU emulsion properties. The best reaction conditions were optimized by taking the viscosity and drop size of the emulsion as two indexes. The reaction scheme of the MWPU was illustrated in [Scheme 2](#).

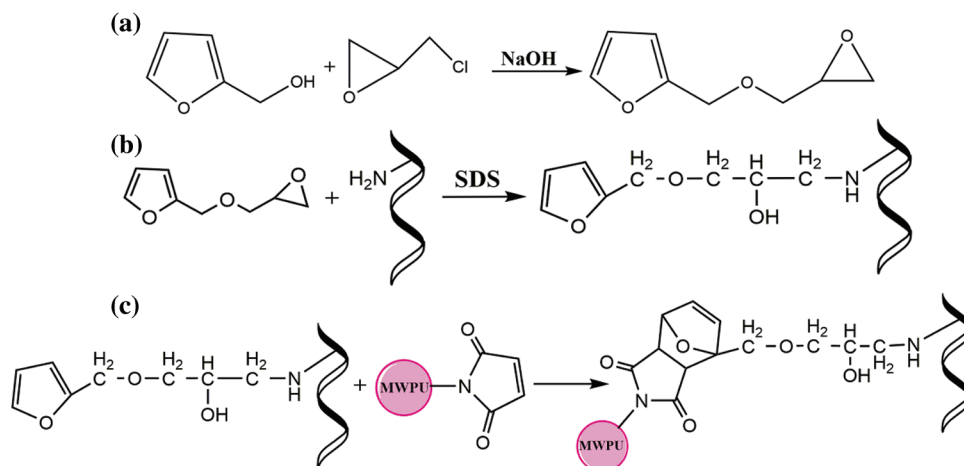


Scheme 2: Reaction scheme to synthesize MWPU

2.3 Preparation of the FGE/GE

The furfuryl glycidyl ether (FGE, [Scheme 3a](#)) was synthesized in previous research [44]. ECH (101.77 g, 1.1 mol) and tetrabutylammonium bisulfate (4.00 g) were added into a 500 ml flask and stirred thoroughly. FA (98.10 g, 1.0 mol) was slowly dropped into the reaction systems and then reacted for 4 h. The NaOH aqueous (160 mL, 50 wt.%) was dropped into the solution at a constant speed within 30 min and then reacted for 2 h. It should be noted that the temperature of the entire reaction system does not exceed 10°C. The crude product was washed three times with distilled water. The organic layer was collected, which was extracted with Diethyl ether anhydrous several times until the pH of the aqueous phase was neutral, and the oil phase was the prepared FGE.

GE was soaked in distilled water at room temperature for 30 min in a three-necked round-bottomed flask, then heated and stirred for 30 min at 40°C to obtain GE hydrolysate. The pH of the GE hydrolysate was adjusted to 8 by 10 wt.% NaOH solution was allowed to stand for 30 min to obtain the GE alkaline hydrolysate. Then, SDS was added to the reactants and mixed well, then FGE was dripped and reacted at 60°C for 2 h to obtain epoxy compound modified gelatin (FGE/GE). The reaction scheme of the FGE/GE was illustrated in [Scheme 3b](#).



Scheme 3: (a) Synthetic route of FGE. (b) Synthetic route of FGE/GE. (c) Synthetic route of MWPU-FGE/GE adhesive

2.4 Preparation of the MWPU-FGE/GE Adhesive

The MWPU-FGE/GE adhesive was prepared by directly mixing MWPU and FGE/GE with the weight ratio of 20:1, 15:1, 10:1, 5:1, 1:1, 1:5, 1:10, 1:15, and 1:20. The mixture with MWPU was pre-crosslinked at 60°C, 65°C, 70°C, 75°C, and 80°C for 24 h obtain MWPU-FGE/GE adhesive. Exploring the effects of different weight ratios and different pre-crosslinking reaction temperatures on adhesion properties. The optimal reaction conditions were optimized in terms of the shear strength and T-peel strength of the MWPU-FGE/GE adhesive. The reaction scheme of the FGE/GE was illustrated in [Scheme 3c](#).

2.5 ¹H-NMR Spectroscopy

The sample of FGE was dissolved in deuteriochloroform (CDCl₃), and the number of the testing was 32 times. The AVANCE NEO 600 MHz nuclear magnetic resonance spectroscopy (Bruker Corporation, Billerica, USA) was used for the ¹H-NMR test.

2.6 FT-IR Spectra

MWPU, FGE/GE, and MWPU-FGE/GE adopted the membrane methods to prepare samples for testing. FGE and FA used spectral purity potassium bromide to prepare samples. The FT-IR tests were performed using a Vertex70 infrared spectrophotometer (Bruker Corporation, Billerica, USA) provided Fourier transform analysis. The number of the testing was 32 times, and the scan range was set from 4000 to 500 cm⁻¹.

2.7 SEM

The films of GE, WPU-GE, and MWPU-FGE/GE adhesives were embrittled to the proper size in nitrogen and then fixed on the aluminum sample table by a conductive adhesive. After spraying gold, the section of the film was observed by FEI Q45 scanning electron microscope (FEI Company, Hillsboro, USA). The acceleration voltage was 10 kV, and the magnification was 2000 times.

2.8 TG

The films of GE, WPU-GE, and MWPU-FGE/GE adhesives (5 mg) were placed in an aluminum pan and heated from 40°C to 600°C at a heating rate of 10 °C/min under N₂ condition. The TGA Q500 thermogravimetric analysis (TA Instruments, Newcastle, USA) was used for the TG test.

2.9 Viscosity Test of MWPU Emulsion

The viscosity of the MWPU emulsion was measured at 25°C with an SNB-1 rotation viscometer (Shanghai Fangrui Instrument Co., Ltd., Shanghai, China).

2.10 Drop Size Test of MWPU Emulsion

The MWPU was diluted to the solids content of 0.1% by deionized water. The drop size of the emulsion was measured by a ZS90 nanoparticle size analyzer (Malvern Instrument, Malvern, UK).

2.11 Solid Content of Adhesives

The solid content of different formulations of adhesives was tested by drying about 1.00 g samples at 105°C until drying to constant weight and calculating the weight ratio of residue to the whole mass.

2.12 Quality Standard Test of Prepared Adhesives

To measure the adhesion properties of the adhesive, the shear strength and T-peel strength of the adhesive were tested by the UTM2012 electronic universal testing machine (Shenzhen Suns Technology Stock Co., Ltd., Shenzhen, China).

(1) Test of the shear strength

The shear strength was tested according to the standard GB/T 7124-2008. Before the test, applied an appropriate amount of modified adhesive evenly on the skin, activated it at 60°C for 4 min, and bonded it. The length of the bonding surface was $12.5 \text{ mm} \pm 0.25 \text{ mm}$, and the separation speed of the specimen holder was $25 \text{ mm/min} \pm 2 \text{ mm/min}$.

(2) Test of the T-peel strength

The T-peel strength was tested according to the standard GB/T 532-2008. Before the test, applied an appropriate amount of modified adhesive evenly on the skin, activated it at 60°C for 4 min, and bonded it. Fixed the sample on the universal testing machine so that the peeling angle was about 180°. The adhesive area of $100 \times 25 \text{ mm}^2$ and the separation speed of the sample holder was $50 \text{ mm/min} \pm 5 \text{ mm/min}$.

3 Results and Discussion

3.1 Synthesize of MWPU Emulsion

The monomer content of the MWPU was optimized by the viscosity of the MWPU solution (Fig. 1). The effect of the R-value (Isocyanate index, $n_{\text{NCO}}: n_{\text{OH}}$) on the viscosity of MWPU and the drop size of the emulsion was shown in Figs. 1a and 1b. The viscosity of the MWPU emulsion first increased and then decreased with the increase of the R-value. The drop size of the emulsion firstly remains almost unchanged, decreased sharply, then increased. At the small R-value, the relatively high hydrophilicity of the MWPU made the polymer chains in a relatively extended state and resulted in a large emulsion drop size. With the increase of R-value, the hard segment content of MWPU chains increases, which results in the increased viscosity of the emulsion. The emulsion drop size intends to decrease with the rise of the hydrophobicity and grow with the growth of the rigidity of the MWPU molecular. At the R-value of 1.8, the viscosity of the emulsion reached the maximum value while the drop size of the emulsion reached the minimum value. When the hard segment content continued to increase, the relatively high hydrophobicity promoted the further aggregation of the tiny droplets to minimize the surface energy and resulted in the increased drop size and decreased viscosity.

The effect of DMPA (wt.%, based on the weighted sum of IPDI and PTMG) content and TEA (% based on the amount of DMPA) content on the viscosity of MWPU and the drop size of the emulsion was shown in Figs. 1c–1f. With the increase of DMPA content and TEA content, the change in MWPU emulsion viscosity and drop size was similar to that of the R-value. The decrease of the drop size of the emulsion with the

increase of DMPA content is due to the DMPA containing the acetate group, which helps to stabilize the emulsion by electrostatic repulsion. With the rise of DMPA content, the hydrophilicity and molecular weight of the WPU increases, resulting in increased chain entanglement and viscosity. With further growth of the DMPA, the high tangles cause difficulties in the dispersion of the emulsion drops and result in increased drop size and decreased viscosity. TEA was used to neutralize the $-\text{COOH}$ introduced to MWPU chains after the hydrophilic chain extension by DMPA. As the TEA was increased, the molecular ionization firstly increased and then decreased, resulting in the first decrease and then increase of the emulsion drop size. As the molecular ionization increases, and the hydrophilicity increases, the MWPU emulsion viscosity increases. When the concentration of DMPA was 5%, and the concentration of TEA was 100%, the viscosity of MWPU emulsion was the maximum value, and the drop size of emulsion reached the minimum value.

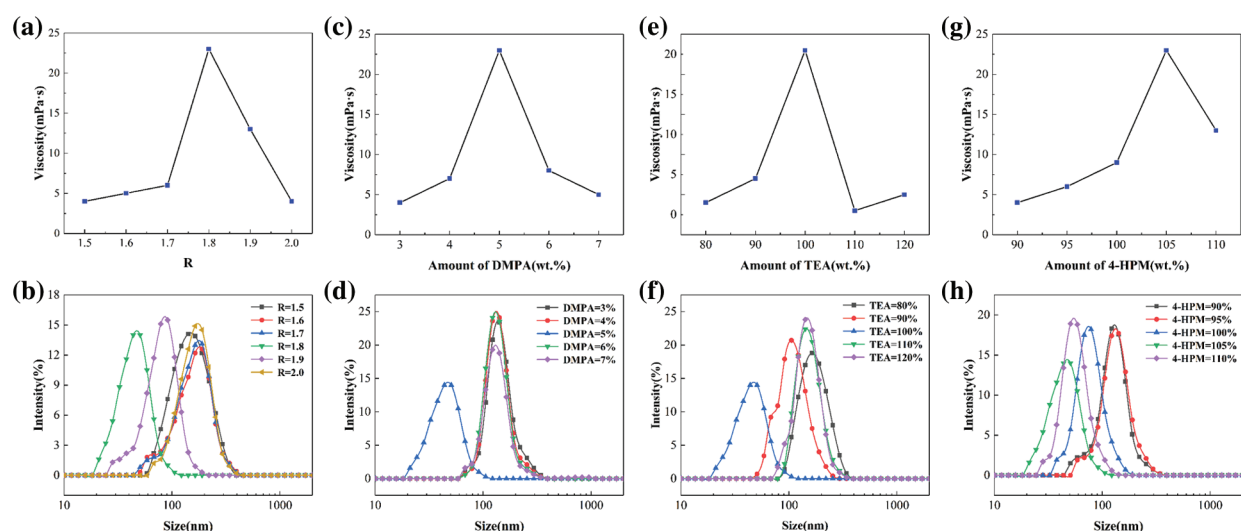


Figure 1: The influences of different monomer content on the viscosity of MWPU emulsion. (a) R-value, (c) DMPA content, (e) TEA content, (g) 4-HPM content. The influences of different monomer content on the drop size of MWPU emulsion. (b) R-value, (d) DMPA content, (f) TEA content, (h) 4-HPM content

The viscosity of the MWPU emulsion first increased and then decreased with the increase of 4-HPM (%), based on the amount of theoretical $-\text{NCO}$ (Fig. 1g). The drop size of the emulsion firstly remains almost unchanged, decreased mildly, then increased (Fig. 1h). During the preparation of MWPU, whether the $-\text{NCO}$ group can completely react with the $-\text{OH}$ group in 4-HPM monomer was the key to determining the degree of blocking. When 4-HPM was slightly excessive, $-\text{NCO}$ was completely reacted and blocked completely. The molecular chains were entangled by hydrogen bonding, which increased the viscosity of the emulsion and decreased the drop size (Fig. 1h). When the content of the 4-HPM was too high, part of the monomer did not participate in the reaction. The molecular weight of the polymer no longer increased and the viscosity of the emulsion decreased. Therefore, when the mass concentration of 4-HPM was 105%, the viscosity of the MWPU emulsion reached the highest value.

The successful synthesis of the MWPU was confirmed by the FTIR test. The FTIR spectrum of MWPU was shown in Fig. 2. The 3330 cm^{-1} peaks belonged to the N–H stretching vibration absorption peak. The peaks at 2940 cm^{-1} and 2852 cm^{-1} belonged to the asymmetric stretching vibration peak and the symmetric stretching vibration peak of C–H. The peak at 1700 cm^{-1} belonged to the C=O stretching vibration absorption peak of carbamate. The peak at 1365 cm^{-1} belonged to the C–N stretching vibration

absorption peak of the imide group. At the same time, the peaks at 1130 cm^{-1} and 775 cm^{-1} belonged to the lateral and out-of-plane bending vibration absorption peaks of the imide ring. It showed that 4-HPM was introduced into the molecular chain of WPU. However, there was no absorption peak at 2270 cm^{-1} , indicating that $-\text{NCO}$ had been wholly reacted.

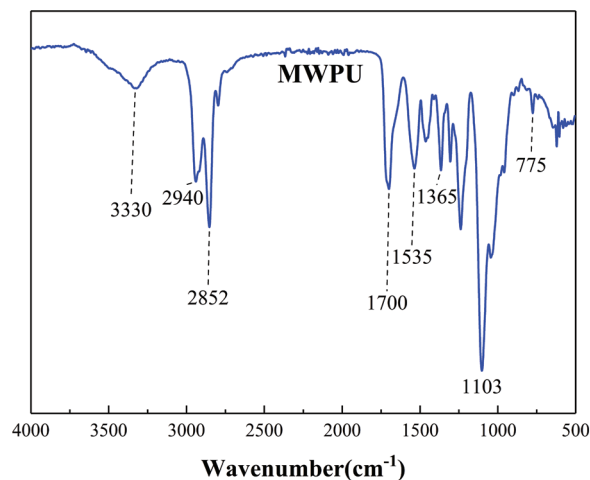


Figure 2: The FT-IR spectrum of MWPU

3.2 Synthesis of FGE

The FGE was synthesized according to the experimental section, and the chemical structure of FGE was examined by the $^1\text{H-NMR}$ test. As shown in Fig. 3a, the $-\text{O-CH=C-}$ (a) connected to the furan ring corresponds to a signal of 7.52 ppm, and the signal corresponding to the $=\text{CH-CH=}$ (b and c) on the furan ring was 6.50 ppm. The connection to the methylene group (d) adjacent to the furan ring corresponded to a signal of 4.52 ppm. At the same time, the methylene group (e) connected to the epoxy group corresponded to the sign of 3.74 and 3.55 ppm, and the methine group (f) linked to the epoxy ring corresponded to the sign of 3.46 ppm. The methylene group was connected to the ring The methylene group (g) of the oxygen ring corresponded to signals of 2.80 and 2.62 ppm. Thus, the FGE was synthesized successfully. The obtained FGE was used to graft on GE to form the FGE/GE.

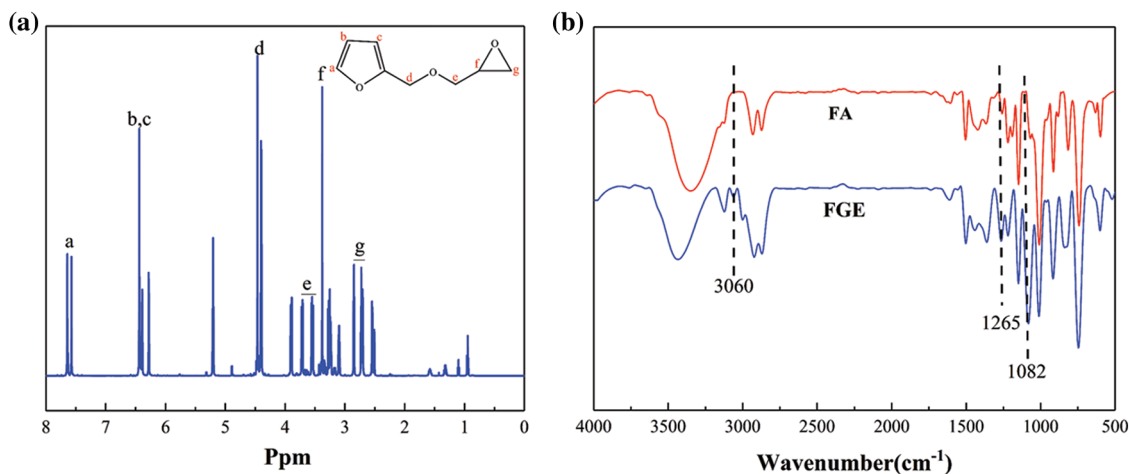


Figure 3: The (a) $^1\text{H-NMR}$ and (b) FT-IR spectrum of FGE

As shown in Fig. 3b, the peak at 3060 cm^{-1} belonged to the C–H stretching vibration absorption peak in the epoxy ring of FGE, and the peak at 1265 cm^{-1} belonged to the stretching vibration absorption peak of C–O–C on the FGE epoxy ring. The peak at 1082 cm^{-1} belonged to the stretching vibration absorption peak on the ether bond C–O–C on the FGE. These peaks were all characteristic peaks of FGE, indicating that FGE was successfully prepared.

3.3 The Synthesis of MWPU-FGE/GE Adhesive

The MWPU-FGE/GE adhesive was synthesized by the pre-crosslinking of FGE/GE with MWPU through DA cycloaddition reaction. The chemical structure of FGE was monitored by the FT-IR spectrum (Fig. 4). The characteristic peaks of gelatin appeared in FGE/GE and MWPU-FGE/GE, including the amide I band (C=O stretching vibration) absorption peak at 1660 cm^{-1} and the amide II band (C–N–H bending vibration) absorption peak at 1530 cm^{-1} , and the amide III band (C–N stretching vibration) absorption peak at 1238 cm^{-1} . The difference was that the C–O stretching vibration absorption peak (1100 cm^{-1}) of the furan ring of FGE/GE disappeared, while the C=O stretching vibration absorption peak (1730 cm^{-1}) of the carbamate appeared in MWPU-FGE/GE. These showed that MWPU and FGE/GE had successfully reacted.

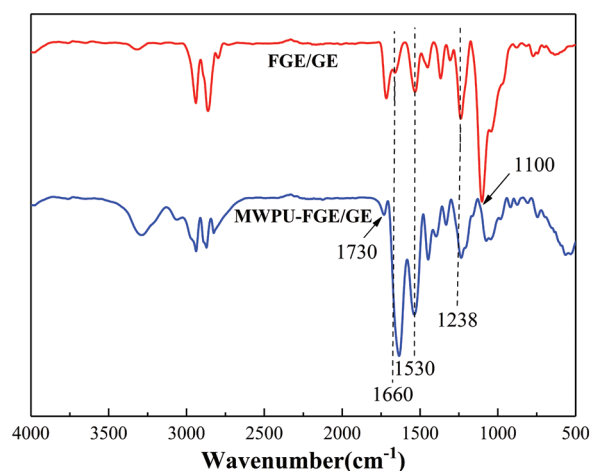


Figure 4: The FT-IR spectrum of FGE/GE and MWPU-FGE/GE

3.4 Effect of Reaction Conditions on Adhesion Properties of MWPU-FGE/GE Adhesive

The monomer content and reaction conditions highly affected the adhesion properties of the MWPU-FGE/GE adhesive (Fig. 5). The shear strength and T-peel strength were used to characterize the adhesion strength of the adhesive towards the skin. As shown in Figs. 5a and 5b, the shear strength and T-peel strength of the adhesive first increased and then decreased with the increase of GE and FGE content (wt.%, based on the weight of GE). And the adhesion properties of the modified adhesive first increased and then decreased with the increase of the weight ratio of FGE/GE to MWPU (Fig. 5c). This might be because the adhesive was caused by the furan group (electron-rich diolefin) of FGE/GE and the maleimide group (electron-deficient diolefin) of MWPU reacted DA reaction to obtain initial curing. Both excess and deficiency of gelatin or FGE would cause the inadequate grafting of FGE in GE and result in the relatively low cross-linking degree of the cured MWPU-FGE/GE adhesive. On the other hand, the increase of GE content would cause the rise in the viscosity of adhesive, which will hinder the penetration of adhesive into the skin and result in decreased adhesion strength. Therefore, the concentration of GE and FGE should be 15% and 25%, and the weight ratio of FGE/GE to MWPU should be 10:1.

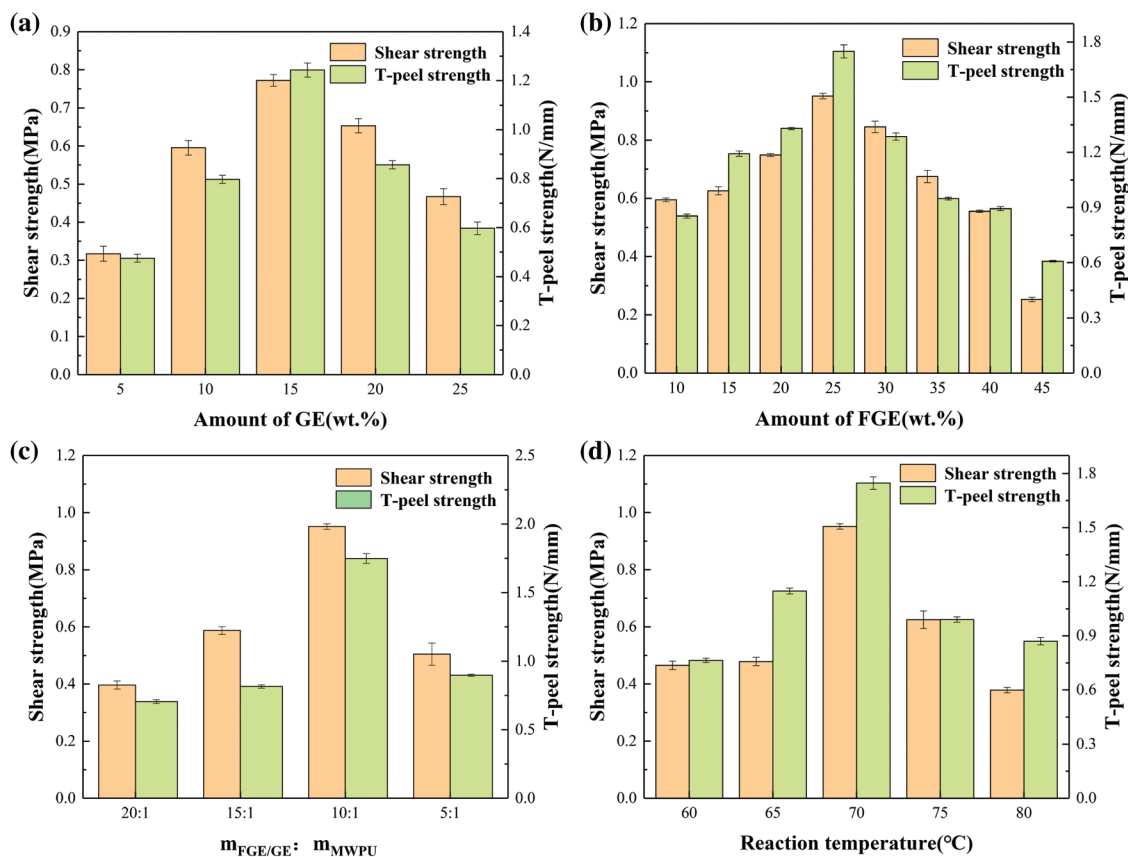


Figure 5: The influences of different monomer content and different reaction conditions on the adhesion properties of the MWPU-FGE/GE adhesive. (a) GE content, (b) FGE content, (c) the weight ratio of FGE/GE to MWPU, (d) reaction temperature

With the increase of reaction temperature, the shear strength and T-peel strength of the modified adhesive first increased and then decreased (Fig. 5d). This might be because as the reaction temperature increased and the collision probability of the monomer increased, the reaction activity increased, and the degree of cross-linking of the cured adhesive improved. So, the adhesion strength of the modified adhesive increased. However, the DA cycloaddition reaction had the characteristics of thermal reversibility. If the reaction temperature was too high, some modified adhesives would undergo a DA reverse reaction, resulting in a decrease in the degree of cross-linking of the emulsion, and therefore, the adhesion strength decreased.

3.5 Effect of Different Curing Conditions on Adhesion Properties of MWPU-FGE/GE Adhesive

Since the curing time and curing temperature highly affects the cross-links introduced by the DA cycloaddition reaction and the water evaporation, the effect of the curing temperature and time on the adhesion strength of the MWPU-FGE/GE adhesive were then investigated (Fig. 6). The shear strength and T-peel strength of the modified adhesive increased with the increase of curing time when the curing temperature was room temperature, 40°C, and 50°C, respectively (Fig. 6a). With the curing time increased, such increase of the adhesive strength was the combined result of the gradual evaporation of water, and the increased cross-linking density, as the evaporation of water, would cause the increase of chain density and with the elongation of the reaction time, more DA reaction would take place to cross-link MWPU and FGE/GE. Due to the short curing time, the evaporation of water was limited.

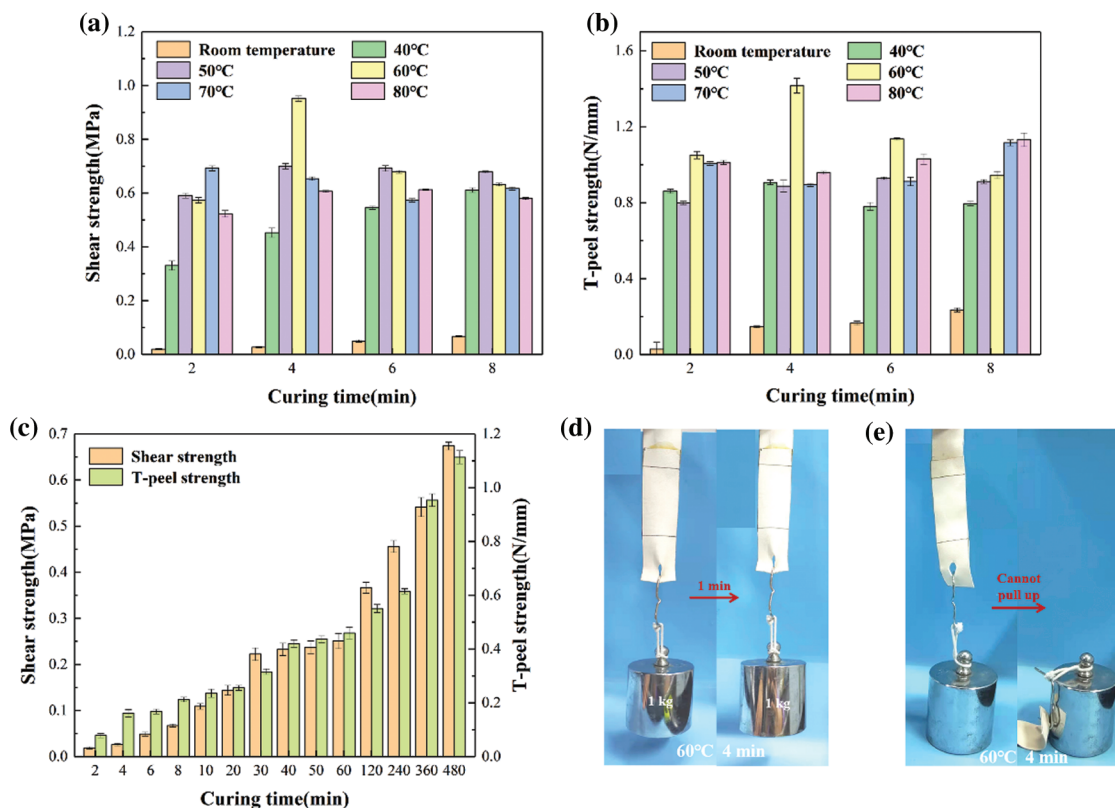


Figure 6: The influences of the curing time and temperature on the (a) shear strength and (b) T-peel strength of MWPU-FGE/GE adhesive. (c) The influences of the curing time at room temperature on the adhesion properties of MWPU-FGE/GE adhesive. Curing at 60°C for 4 min, the (d) MWPU-FGE/GE adhesive could, (e) WPU-GE adhesive could not hold the weight of 1 kg

At this time, the shear strength and T-peel strength of the modified adhesive were mainly caused by the cross-linking of the DA reaction. When the curing temperature was over 60°C, the adhesion strength reached relatively a high value with the shear strength and T-peeling strength of 0.5734 MPa and 1.0506 N/mm, respectively, at a short curing time of 2 min. Then, the adhesion strength firstly increased slightly, then decreased with the increase of curing time. This resulted from the fast evaporation of water at high temperatures and the degradation of gelatin, and the DA reverse reaction at high temperature. Similarly, at the same curing time, the adhesion strength firstly increased and then decreased with the increase of the curing temperature. When the curing temperature increased from room temperature to 40°C, the adhesion strength increased sharply. This might be because the skin was a porous material with a large number of pores and skin fibers on the surface. When the temperature was low, the formation of the helix junctions between gelatin chains highly constrained the movement of the chains and resulted in the high viscosity of the MWPU-FGE/GE adhesives which hindered the penetration of the adhesive to the pores and from interlock with skin. The viscosity decreased as the temperature increased to 40°C, and the adhesive could infiltrate into the pores of the skin and form interlock with skin, which highly increased the adhesion strength. As shown in Figs. 6d and 6e, the adhered skin (cured at 60°C for 4 min) could hold the weight of 1 kg tightly for over 1 min without slip, while the WPU-GE adhesive could not hold much weight at prolonged curing time of 4 min or increased the curing temperature of 60°C.

The adhesion strength of MWPU-FGE/GE adhesives could be enhanced by elongating the curing time at room temperature. The shear strength and T-peel strength of the modified adhesive gradually increased as the

curing time increased and reached a similar value with those cured at 60°C for 6 min or room temperature for 480 min (Fig. 6c). This might be because, at room temperature, the infiltration effect of the modified adhesive on the skin surface became poor. On the other hand, the MWPU-FGE/GE adhesive was an aqueous system. At room temperature, the volatilization of water molecules was slower, and the impact of effective molecules in the system was less. Therefore, the adhesion properties of MWPU-FGE/GE adhesive were poor. At this time, prolonging the curing time of the adhesive would increase the collision of molecules, so the shear strength and T-peel strength could be improved.

3.6 Effect of Different Formulations on the Solid Content of Adhesives

Solid content is an important indicator for evaluating water-based adhesives. Generally speaking, the higher the solid content, the better the adhesion properties of the water-based adhesive. The comparison of the solid content of different formulations of adhesives were shown in Fig. 7. It can be seen that the modified gelatin by WPU resulted in a limited increase of 8.28% in the solid content. This may be because WPU and gelatin are mainly bonded through interaction forces such as hydrogen bonding, which results in a slight improvement of the stability of the adhesive emulsion and precipitate appears at the bottom of the WPU-GE emulsion after a waiting time of several days. The solid content of the MWPU-FGE/GE increases by 14.9%. This is probably because the cross-linking reaction between the FEG/GE and MWPU through the DA cycloaddition reaction between MWPU and FGE improves the stability of the emulsion and the MWPU-FGE/GE emulsion with a high solid content of 28.67% is stable after a long storage period.

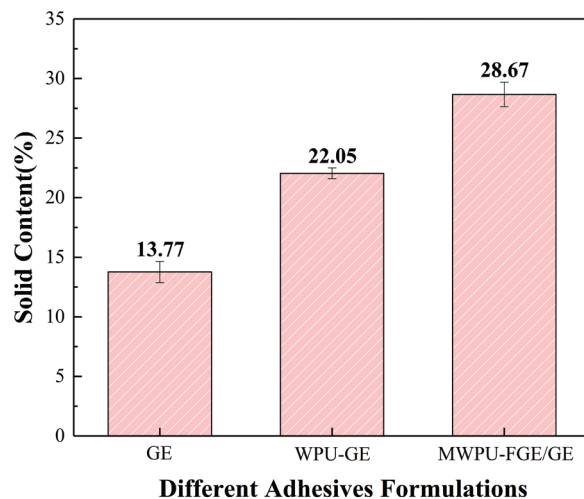


Figure 7: The comparison of the solid content of different adhesives

3.7 Effect of Curing at Room Temperature on the Adhesion Properties of Different Adhesives

Under the curing condition of room temperature and the curing time of 480 min, the adhesion properties of different adhesives were compared by the shear and T-peel strength of the adhesive (Fig. 8). The adhesion properties of the WPU-GE adhesive without the DA cycloaddition reaction functional groups at room temperature were detected to investigate the effect of DA cycloaddition reaction on the adhesion properties. It could be seen that the adhesion properties of WPU-GE adhesives at room temperature were poor, and the adhesion strength was improved with the increase of the curing time. However, the WPU-GE adhesive exhibited much lower adhesion strength at room temperature than the MWPU-FGE/GE adhesive. At curing time up to 480 min, the shear and T-peel strength were only 0.1710 MPa and 0.2443 N/mm, which were much lower than those of the sample adhered by the MWPU-FGE/GE

adhesive. It can be seen that the commercial water-based adhesive could not achieve adequate bonding between the skin pieces at room temperature either.

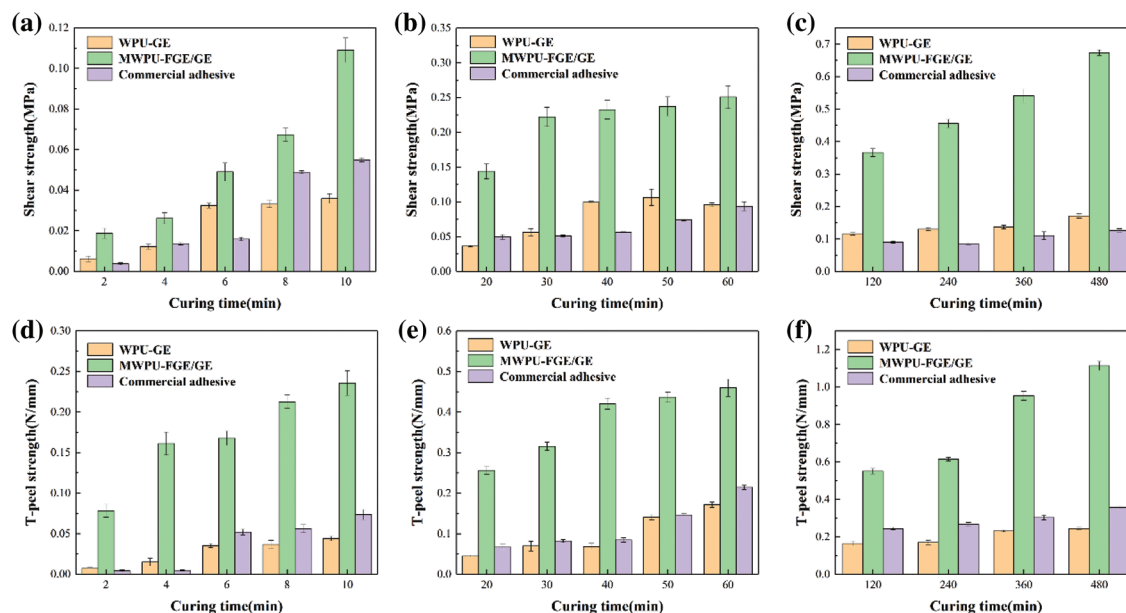


Figure 8: The influences of curing for (a) 10 min, (b) 40 min, (c) 480 min on the shear strength of different adhesives at room temperature. The influences of curing for (d) 10 min, (e) 40 min, (f) 480 min on the T-peel strength of different adhesives at room temperature

3.8 SEM

Fig. 9 was a segment of the GE, WPU-GE, MWPU-FGE/GE film, respectively. The fracture surface of GE film (Fig. 9a) was smooth, indicating a typical brittle fracture.

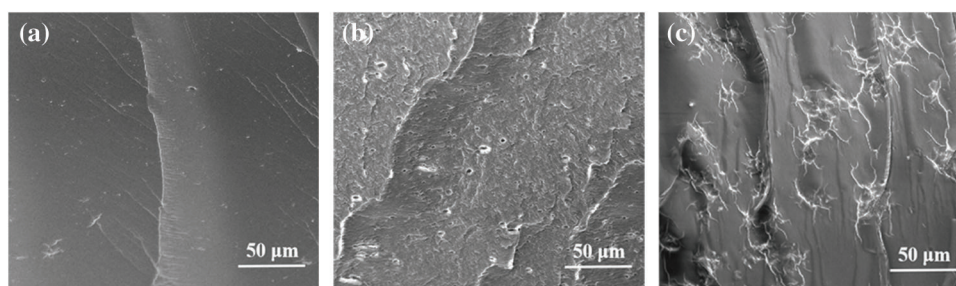


Figure 9: The SEM images of GE adhesive and the modified adhesives. (a) GE adhesive, (b) WPU-GE adhesive, (c) MWPU-FGE/GE adhesive

As shown in Fig. 9b, the WPU-GE section exhibited more microcracks, fewer large cracks, indicating that it was tough. This might be because the hard segments in the WPU molecular chain were formed of a urethane group and a urea group, and there was a strong hydrogen bond between the same. The soft segment was mainly C–O and C–C in the polyether block in the molecular chain, which was randomly curly. During the curing process, the hard segment was easy to collect together, producing several micro-zone distributions in the soft section forming microphase separation. The addition of WPU improved GE toughness and

increased its shear strength. Comparative Figs. 9b and 9c could be apparent that the WPU-GE adhesive section exhibited a dispersed phase, and the gelatin-based adhesive prepared by MWPU modification FGE/GE could form a uniform phase. Thus, a relatively smooth section with a compact structure was formed.

3.9 TG

The thermal stability of the cured MWPU-FGE/GE adhesive was studied by the TG test. TG curves and DTG curves of gelatin, WPU-GE, and MWPU-FGE/GE adhesive are shown in Fig. 10. These three adhesives have a slight weight loss process at 120°C, which was mainly due to the thermal decomposition of moisture and evaporation of the volatile solvent in the adhesive. After the introduction of MWPU and FGE in gelatin, the active group ($-\text{NH}_2$, $-\text{OH}$) on the gelatin chain formed a cross-linking structure, and the adhesive molecule cohesion was improved. During thermal decomposition, in addition to the amide bonds on the gelatin chain needing to be broken, there was a need to fracture of the ring structure formed by the bilateral hydrocarbon group, and the cross-links formed between the epoxy group and the amino group, which required more energy, thereby increasing the thermal stability of the product. It can be seen from Fig. 10a that the minimum weight reduction in the weight of the MWPU-FGE/GE adhesive is within 120°C. The maximum decomposition temperature of the adhesive was between 300°C and 350°C.

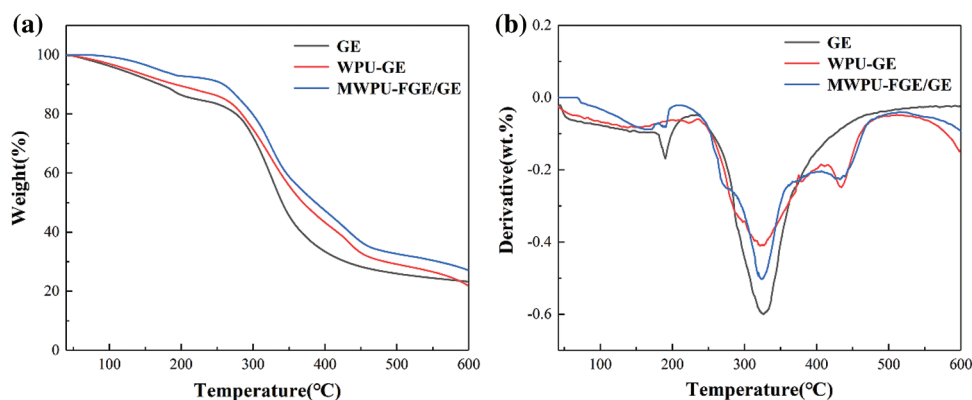


Figure 10: (a) TG curves and (b) DTA curves of different adhesives

4 Conclusions

The current increasing awareness of environmental protection has promoted the design and research of new biomass-based adhesives. Gelatin, as a biomass material that can be extracted from waste dander, can be used to prepare adhesives not only to maximize the use of resources but also to enhance the practical value and economic benefits of gelatin. In this research, by introducing DA cycloaddition reaction in the click chemistry, a novel water-based adhesive (MWPU-FGE/GE adhesive) with low temperature curing property was developed. The polymers containing the functional groups for the DA cycloaddition reaction (FGE/GE and MWPU) were successfully synthesized by grafting FGE on gelatin and end-capping WPU by 4-HPM. Due to the formation of DA reaction, the degree of cross-linking density of gelatin was successfully increased and enhanced the adhesion strength of gelatin meets the industrial application requirement and a certain extent reduced the emission of harmful substances. When the MWPU-FGE/GE adhesive was applied to the skin surface, the adhesion performances at moderate temperature were significantly improved and exceeded some of the water-based commercially available adhesives. Therefore MWPU-FGE/GE emulsion has excellent application potential as a green adhesive.

Funding Statement: The authors are grateful for the financial support from the National Natural Science Foundation of China (22002079, 2207081675, and 22108165), and the Natural Science Basic Research Program of Shaanxi (Program No. 2021JQ-548).

Conflicts of Interest: The authors declare that they have no conflicts of interest to report regarding the present study.

References

1. Sathish, M., Madhan, B., Raghava, R. J. (2019). Leather solid waste: An eco-benign raw material for leather chemical preparation-A circular economy example. *Waste Management*, 87(6), 357–367. DOI 10.1016/j.wasman.2019.02.026.
2. Wang, L., Li, J., Jin, Y., Chen, M., Luo, J. et al. (2019). Study on the removal of chromium (III) from leather waste by a two-step method. *Journal of Industrial and Engineering Chemistry*, 79, 172–180. DOI 10.1016/j.jiec.2019.06.030.
3. Lai, J. Y., Li, Y. T. (2010). Functional assessment of cross-linked porous gelatin hydrogels for bioengineered cell sheet carriers. *Biomacromolecules*, 11(5), 1387–1397. DOI 10.1021/bm100213f.
4. Liu, H., Zhao, W., Gao, G., Ren, X. (2019). Tough, anti-freezing and non-drying double network organohydrogels. *Materials Today Communications*, 21(32–33), 100609. DOI 10.1016/j.mtcomm.2019.100609.
5. Schreiber, R., Gareis, H. (2007). *Gelatine handbook: Theory and industrial practice*. England: John Wiley & Sons.
6. Khodaei, D., Oltrogge, K., Hamidi-Esfahani, Z. (2020). Preparation and characterization of blended edible films manufactured using gelatin, tragacanth gum and, Persian gum. *LWT*, 117(1526), 108617. DOI 10.1016/j.lwt.2019.108617.
7. Moosavi, S. M. R., Zerafat, M. M. (2021). Fabrication of Gelatin-based natural nanocomposite films using nanoclay and Chitosan for food packaging applications. *International Journal of Nano Dimension*, 12(4), 343–354.
8. Ciannanea, E. M., Castillo, L. A., Barbosa, S. E., De-Angelis, M. G. (2018). Barrier properties and mechanical strength of bio-renewable, heat-sealable films based on gelatin, glycerol and soybean oil for sustainable food packaging. *Reactive and Functional Polymers*, 125(7), 29–36. DOI 10.1016/j.reactfunctpolym.2018.02.001.
9. Elkhoully, H., Mamdouh, W., El-Korashy, D. I. (2021). Electrospun nano-fibrous bilayer scaffold prepared from polycaprolactone/gelatin and bioactive glass for bone tissue engineering. *Journal of Materials Science: Materials in Medicine*, 32(9), 1–15. DOI 10.1007/s10856-021-06588-6.
10. Swetha, S., Balagangadharan, K., Lavanya, K., Selvamurugan, N. (2021). Three-dimensional-poly (lactic acid) scaffolds coated with gelatin/magnesium-doped nano-hydroxyapatite for bone tissue engineering. *Biotechnology Journal*, 16(11), 2100282. DOI 10.1002/biot.202100282.
11. Behtouei, E., Zandi, M., Askari, F., Daemi, H., Zamanlui, S. et al. (2021). Bead-free and tough electrospun PCL/gelatin/PGS ternary nanofibrous scaffolds for tissue engineering application. *Journal of Applied Polymer Science*, 139(2), 51471. DOI 10.1002/app.51471.
12. Das, R. P., Gandhi, V. V., Singh, B. G., Kunwar, A. (2021). Balancing loading, cellular uptake, and toxicity of gelatin-pluronic nanocomposite for drug delivery: Influence of HLB of pluronic. *Journal of Biomedical Materials Research Part A*, 110(2), 304–315. DOI 10.1002/jbm.a.37287.
13. Cao, S., Li, L., Du, Y., Gan, J., Wang, J. et al. (2021). Porous gelatin microspheres for controlled drug delivery with high hemostatic efficacy. *Colloids and Surfaces B: Biointerfaces*, 207(20), 112013. DOI 10.1016/j.colsurfb.2021.112013.
14. Li, M., Li, J. P., Wang, Y. S., He, Q. (2021). Construction and anti-tumor effect evaluation of a dual-responsive hyaluronic acid carbon quantum dot-gelatin nano-drug delivery system. *Journal of Sichuan University: Medical Science Edition*, 52(4), 577–584. DOI 10.12182/20210760103.
15. Qin, Z., Dong, D., Yao, M., Yu, Q., Sun, X. et al. (2019). Freezing-tolerant supramolecular organo-hydrogel with high toughness, thermoplasticity, and healable and adhesive properties. *ACS Applied Materials & Interfaces*, 11(23), 21184–21193. DOI 10.1021/acsami.9b05652.

16. Dorr, D., Frazier, S., Hess, K., Traeger, L., Srubar, W. III (2015). Bond strength of biodegradable gelatin-based wood adhesives. *Journal of Renewable Materials*, 3(3), 195–204. DOI 10.7569/JRM.2015.634108.
17. Zhao, Q., Mu, S., Long, Y., Zhou, J., Chen, W. et al. (2019). Tannin-tethered gelatin hydrogels with considerable self-healing and adhesive performances. *Macromolecular Materials and Engineering*, 304(4), 1800664. DOI 10.1002/mame.201800664.
18. Wang, B., Yang, C., Wang, J., Xia, S., Wu, Y. (2019). Effects of combined pullulan polysaccharide, glycerol, and trehalose on the mechanical properties and the solubility of casted gelatin-soluble edible membranes. *Journal of Food Processing and Preservation*, 43(1), e13858. DOI 10.1111/jfpp.13858.
19. Dang, X., Yuan, H., Shan, Z. (2018). An eco-friendly material based on graft copolymer of gelatin extracted from leather solid waste for potential application in chemical sand-fixation. *Journal of Cleaner Production*, 188, 416–424. DOI 10.1016/j.jclepro.2018.04.007.
20. Shi, J., Chen, S., Wang, L., Zhang, X., Gao, J. et al. (2018). Rapid endothelialization and controlled smooth muscle regeneration by electrospun heparin-loaded polycaprolactone/gelatin hybrid vascular grafts. *Journal of Biomedical Materials Research Part B: Applied Biomaterials*, 107(6), 2040–2049. DOI 10.1002/jbm.b.34295.
21. Zhang, L., Liu, J., Zheng, X., Zhang, A., Zhang, X. et al. (2019). Pullulan dialdehyde crosslinked gelatin hydrogels with high strength for biomedical applications. *Carbohydrate Polymers*, 216(1), 45–53. DOI 10.1016/j.carbpol.2019.04.004.
22. Wazarkar, K., Sabnis, A. (2018). Synergistic effect of P S and crosslink density on performance properties of epoxy coatings cured with cardanol based multifunctional carboxyl curing agents. *Reactive and Functional Polymers*, 128, 74–83. DOI 10.1016/j.reactfunctpolym.2018.04.016.
23. Wang, X., Zhu, J., Liu, X., Zhang, H. J., Zhu, X. (2020). Novel gelatin-based eco-friendly adhesive with a hyperbranched cross-linked structure. *Industrial & Engineering Chemistry Research*, 59(13), 5500–5511. DOI 10.1021/acs.iecr.9b06822.
24. Wongsamut, C., Suwanpreedee, R., Manuspiya, H. (2020). Thermoplastic polyurethane-based polycarbonate diol hot melt adhesives: The effect of hard-soft segment ratio on adhesion properties. *International Journal of Adhesion and Adhesives*, 102(6), 102677. DOI 10.1016/j.ijadhadh.2020.102677.
25. Li, R., Ton, L. J. A., Shan, Z. (2019). The varying mass ratios of soft and hard segments in waterborne polyurethane films: Performances of thermal conductivity and adhesive properties. *European Polymer Journal*, 112, 423–432. DOI 10.1016/j.eurpolymj.2019.01.025.
26. Noreen, A., Zia, K. M., Zuber, M., Tabasum, S., Saif, M. J. (2015). Recent trends in environmentally friendly water-borne polyurethane coatings: A review. *Korean Journal of Chemical Engineering*, 33(2), 388–400. DOI 10.1007/s11814-015-0241-5.
27. Dang, X., Li, Y., Yang, M. (2019). Biodegradable waterborne polyurethane grafted with gelatin hydrolysate via solvent-free copolymerization for potential porous scaffold material. *Journal of the Mechanical Behavior of Biomedical Materials*, 52(10), 79–89. DOI 10.1016/j.jmbbm.2019.01.005.
28. Chowdhury, R. A., Clarkson, C. M., Shrestha, S., El Awad Azrak, S. M., Mavlan, M. et al. (2019). High-performance waterborne polyurethane coating based on a blocked isocyanate with cellulose nanocrystals (CNC) as the polyol. *ACS Applied Polymer Materials*, 2(2), 385–393. DOI 10.1021/acsapm.9b00849.
29. Wang, R., Li, C., Jiang, Z., Wang, Z. (2020). Self-assembly of amphiphilic linear-dendritic carbosilane block surfactant for waterborne polyurethane coating. *Polymers*, 12(6), 1318. DOI 10.3390/polym12061318.
30. Yin, Q., Wang, X., Chen, J., Wu, X., Zheng, J. (2019). Synthesis of blocked waterborne polyurethane with 3,5-dimethylpyrazole for industrial application in digital inkjet printing. *Journal of Applied Polymer Science*, 136(29), 47765. DOI 10.1002/app.47765.
31. Hartmuth, C. K. G. F. M., Barry, S. K. (2001). Click chemistry: Diverse chemical function from a few good reactions. *Angewandte Chemie*, 40(11), 2004–2011 (International Edition). DOI 10.1002/(ISSN)1521-3773.
32. Pan, L. N., Wang, Q., Sun, J., Yan, C. G. (2021). Intramolecular Diels-Alder reaction of styrene with phenoxy-acrylate for construction of functionalized naphthalenes. *Asian Journal of Organic Chemistry*, 10(10), 2591–2595. DOI 10.1002/ajoc.202100401.

33. Li, W., Wei, H., Liu, Y., Li, S., Wang, G. et al. (2021). Fabrication of novel starch-based composite hydrogel microspheres combining Diels-Alder reaction with spray drying for MB adsorption. *Journal of Environmental Chemical Engineering*, 9(5), 105929. DOI 10.1016/j.jece.2021.105929.
34. Debone, P. R., Brandt, J. V., Carvalho dos, S. C., Fernando, C. M. R., Jafelicci, J. M. (2020). Gelatin/dextran-based hydrogel cross-linked by Diels-Alder click chemistry: The swelling and potassium diclofenac releasing. *Medical Devices & Sensors*, 4(1), e10151. DOI 10.1002/MDS3.10151.
35. Tasdelen, M. A. (2011). Diels-Alder click reactions: Recent applications in polymer and material science. *Polymer Chemistry*, 2(10), 2133–2145. DOI 10.1039/c1py00041a.
36. Oluwasanmi, A., Hoskins, C. (2021). Potential use of the Diels-Alder reaction in biomedical and nanomedicine applications. *International Journal of Pharmaceutics*, 604(3), 120727. DOI 10.1016/j.ijpharm.2021.120727.
37. Gevrek, T. N., Sanyal, A. (2021). Furan-containing polymeric materials: Harnessing the Diels-Alder chemistry for biomedical applications. *European Polymer Journal*, 153(22), 110514. DOI 10.1016/j.eurpolymj.2021.110514.
38. Yang, S., Du, X., Deng, S., Qiu, J., Du, Z. et al. (2020). Recyclable and self-healing polyurethane composites based on Diels-Alder reaction for efficient solar-to-thermal energy storage. *Chemical Engineering Journal*, 398, 125654. DOI 10.1016/j.cej.2020.125654.
39. Wu, P., Cheng, H., Wang, X., Shi, R., Zhang, C. et al. (2021). A self-healing and recyclable polyurethane-urea Diels-Alder adduct synthesized from carbon dioxide and furfuryl amine. *Green Chemistry*, 23(1), 552–560. DOI 10.1039/D0GC03695A.
40. Wei, H., Li, W., Chen, H., Wen, X., He, J. et al. (2020). Simultaneous Diels-Alder click reaction and starch hydrogel microsphere production via spray drying. *Carbohydrate Polymers*, 241(1), 116351. DOI 10.1016/j.carbpol.2020.116351.
41. Delplace, V., Nickerson, P. E. B., Ortin-Martinez, A., Baker, A. E. G., Wallace, V. A. et al. (2020). Nonswelling, ultralow content inverse electron-demand Diels-Alder hyaluronan hydrogels with tunable gelation time: Synthesis and *in vitro* evaluation. *Advanced Functional Materials*, 30(14), 1903978. DOI 10.1002/adfm.201903978.
42. Orozco, F., Li, J., Ezekiel, U., Niyazov, Z., Floyd, L. et al. (2020). Diels-Alder-based thermo-reversibly crosslinked polymers: Interplay of crosslinking density, network mobility, kinetics and stereoisomerism. *European Polymer Journal*, 135, 109882. DOI 10.1016/j.eurpolymj.2020.109882.
43. Yeh, C. M., Lin, C. H., Han, T. Y., Xiao, Y. T., Chen, Y. A. et al. (2021). Disulfide bond and Diels-Alder reaction bond hybrid polymers with high stretchability, transparency, recyclability, and intrinsic dual healability for skin-like tactile sensing. *Journal of Materials Chemistry A*, 9(10), 6109–6116. DOI 10.1039/D0TA10135D.
44. Ding, J., Peng, W., Luo, T., Yu, H. (2017). Study on the curing reaction kinetics of a novel epoxy system. *RSC Advances*, 7(12), 6981–6987. DOI 10.1039/C6RA25120J.